nature physics

Perspective

https://doi.org/10.1038/s41567-026-03304-5

An integrated theoretical and numerical approach to understand modern experiments on quantum magnetism

Received: 18 November 2024

Accepted: 17 April 2026

Published online: 29 June 2026

Check for updates

Zi Yang Meng (孟子楊) [1,2] ✉, Cristian D. Batista [3,4] ✉ & Shiliang Li (李世亮) [5,6] ✉

In recent decades, the study of quantum magnets, which feature unconventional behaviour such as exotic quantum phase transitions and quantum spin liquids, and unconventional magnetic states of matter, has made remarkable progress. However, each of the three foundational pillars—numerical simulations, analytical methods and, to a lesser extent, materials synthesis and experiments—often tends to view itself as the primary driver of the field. Even though the need for collaboration among theory, numerics and experiment to understand the complex phases of quantum magnets is well established, in our view there remains a persistent perception from experts in one area that the other two serve merely as supporting tools, primarily useful for validating the dominant ideas of one speciality, and less relevant to shaping the underlying scientific narrative. In this Perspective, we advocate for a different, more integrated approach to overcome the challenges faced by quantum magnetism researchers. We argue that this alternative mindset has already started to advance the understanding of several important quantum magnetic models and their materials realizations.

Quantum magnets have long been a focus for condensed matter research. Theoretical models of spins on a lattice have provided many important physical insights, including predictions of non-trivial quantum effects such as topological order. Substantial experimental efforts have subsequently been dedicated to identifying materials that exhibit such phenomena. These efforts have led to advances on multiple fronts, from the development of new theoretical frameworks to substantial progress in numerical algorithms, simulation techniques, materials synthesis and experimental probes.

Over time, the sophistication and complexity of analytical, numerical and experimental methods has continued to grow. Although in the past each of these approaches to studying quantum magnetism could be pursued independently, substantial advances in understanding now increasingly depend on a combination of experimental and theoretical insights.

This Perspective aims to highlight the growing need for the field of quantum magnetism to pursue an integrated research approach—one that strengthens the synergy among theory, numerical simulation and experiment—and to advocate for a broader appreciation of how such cross-disciplinary collaboration accelerates discovery.

The value of this integrated approach is especially evident in the collective effort to identify and understand exotic phases, including evidence of quantum spin liquids, where quantum fluctuations destroy magnetic order. These phases are expected to exhibit fractionalization, whereby new quasiparticles emerge that carry parts of the fundamental electronic degrees of freedom, such as separate particles carrying

[1]Department of Physics, The University of Hong Kong, Hong Kong, China. [2]State Key Laboratory of Optical Quantum Materials, The University of Hong Kong, Hong Kong, China. [3]Department of Physics and Astronomy, University of Tennessee, Knoxville, TN, USA. [4]Neutron Scattering Division, Oak Ridge National Laboratory, Oak Ridge, TN, USA. [5]Beijing National Laboratory for Condensed Matter Physics, Institute of Physics, Chinese Academy of Sciences, Beijing, China. [6]School of Physical Sciences, University of Chinese Academy of Sciences, Beijing, China. ✉e-mail: zymeng@hku.hk; cbatist2@utk.edu; slli@iphy.ac.cn

only charge or spin, or even a fraction of them. These fractionalized quasiparticles interact among themselves via emergent gauge fields. A major challenge in the search for spin liquids lies in the absence of definitive experimental 'smoking gun' evidence. There have been many efforts to identify clear signatures for fractionalization but very often subsequent research found that they can also be mimicked by other less exotic effects such as disorder. Recent progress has instead relied on the indirect identification of spin-liquid behaviour through quantitative predictions of dynamical properties measured using spectroscopic probes, such as electron spin resonance, scanning tunnelling microscopy and inelastic neutron scattering.

Success in one dimension

The study of quasi-one-dimensional magnets has been an important success story for quantum magnetism, and one where independent theoretical and experimental efforts could make substantial progress. Early field-theoretical work predicted that the constraints of one-dimensional motion mean that the concept of interacting single particles breaks down and is replaced with a so-called Luttinger liquid with fractionalized excitations[1].

The Luttinger liquid concept was validated by comparing theoretical predictions for the dynamical spin structure factor with inelastic-neutron-scattering data on long spin chains[2,3]. A combination of numerical methods with analytical theoretical insights about integrable systems enabled an accurate reproduction of the scattering continuum, including its energy and momentum dependence under different applied magnetic fields.

It is instructive to examine the key factors that enabled the successful discovery and characterization of magnetic Luttinger liquids. The first crucial element was the ability to synthesize quasi-one-dimensional spin systems with an exceptionally low degree of disorder, providing clean experimental platforms where intrinsic quantum effects are not masked by extrinsic factors[4,5].

Second, accurate spin Hamiltonians for theoretical modelling could be constructed because many spin-1/2 chain materials are well described by a nearest-neighbour antiferromagnetic Heisenberg model. This meant that the appropriate model parameters could be easily determined by comparing experimental observation in inelastic-neutron-scattering measurements and model calculations with ab initio methods as well as field theories.

A third important factor was the availability of powerful theoretical tools for computing dynamical spin correlation functions on long chains. These included both analytical methods such as the Bethe ansatz, and numerical techniques such as quantum Monte Carlo (QMC)[6], as well as time-evolution extensions of the density matrix renormalization group (DMRG)[7]. By minimizing both the uncertainty in the underlying spin Hamiltonian and the errors in approximating its dynamics, it became possible to unambiguously reveal the fractionalized nature of the elementary excitations.

It is natural to ask why the same approach has not achieved the same success in the search for spin liquids in two- and three-dimensional materials. Some challenges already emerge in the one-dimensional case[8,9]. Even the well-understood material realizations of Luttinger liquids are quasi-one-dimensional magnets that develop long-range magnetic order at sufficiently low temperatures[4,5]. As a result, the low-energy part of the inelastic-neutron-scattering spectrum features more conventional magnon excitations rather than the continuum of fractionalized excitations predicted by idealized field-theoretic models.

In higher-dimensional materials, all three key ingredients that enabled progress in one dimension become much more challenging. First, the synthesis of low-disorder materials is more difficult, and two- and three-dimensional quantum spin liquids appear to be more sensitive to disorder. This makes it harder to realize clean experimental platforms where intrinsic quantum spin-liquid behaviour can be isolated.

Second, model extraction becomes less reliable, as many spin-liquid candidates in higher dimensions are governed by complex Hamiltonians with multiple competing interactions. Even with the most advanced ab initio methods[10–12], the resulting parameter estimates often carry substantial uncertainties.

Third, the analytical and numerical methods used to probe dynamical properties are generally uncontrolled in the absence of small parameters, or they suffer from systematic limitations. Field-theoretical approaches offer valuable qualitative insights into the long-wavelength behaviour of magnetic systems, but often rely on idealized or oversimplified models. By contrast, the determination of realistic lattice Hamiltonians requires a close integration of theory with experimental data, complemented when possible by advanced ab initio analysis.

Even with a lattice Hamiltonian to hand, numerical schemes face challenges. For example, tensor-network methods suffer from an exponential growth of entanglement, and, except in special cases, QMC simulations are afflicted by the minus-sign problem, in which samples with negative weight make it difficult to perform a convergent calculation.

Faced with such difficulties, we believe that progress in quantum magnetism requires much closer collaboration between disciplines. As the following examples demonstrate, intensive collaborative efforts involving analytical theory, numerics and experiment has led to substantial experimental and theoretical advances in several important quantum magnetic models. We argue that further integration and collaboration is not only essential for quantum magnetism, but also pivotal for advancing the broader field of quantum many-body physics.

Triangular-lattice quantum Ising magnets

The triangular-lattice quantum Ising (TLI) material $TmMgGaO_4$ (TMGO) is, due to its Ising character, a rare case in two dimensions where unbiased, large-scale QMC and thermal tensor renormalization group (TRG) can be performed, which enables very close connections between numerical and specific-heat and inelastic-neutron-scattering measurements[13].

As shown in Fig. 1a, ab initio analysis of the experimental data indicates that TMGO is an Ising-type triangular antiferromagnet[14]. Each Tm^{3+} ion carries a total spin–orbit moment of 6, but the crystal electric field selects a non-Kramers ground-state doublet as the effective magnetic degree of freedom. Because the crystal-field gap between second and third levels is about 400 K (ref. 15), the magnetic ion can be regarded as an effective spin-1/2 moment. The local trigonal crystal field induces an energy splitting Δ within the doublet, which acts as an intrinsic transverse field on the effective spin 1/2 (ref. 14).

Therefore, Tm^{3+} ions contribute highly anisotropic Ising-type moments with $J_z = \pm 6$ along the c axis out of the two-dimensional plane of the triangular lattice, with an effective out-of-plane g factor $g^{zz} \approx 13.2$ (ref. 13). The material is thence described by the TLI model

$$H_{\mathrm{TLI}} = J_1 \sum_{\langle i,j \rangle} S_i^z S_j^z + J_2 \sum_{\langle\langle i,j \rangle\rangle} S_i^z S_j^z - \sum_i \left(\Delta S_i^x + h S_i^z \right), \qquad (1)$$

where $S_i^{x,y,z}$ are the spin operators at site i, the nearest-neighbour (next-nearest-neighbour) coupling is J_1 (J_2), Δ is the energy splitting between the two lowest non-Kramers $\Phi_\pm$ levels, and $h = H^z g^{zz} \mu_B$, with H being the z component of the external magnetic field and μ_B the Bohr magneton.

The generic phase diagram of the TLI model (Fig. 1b) is well established in the field-theoretical and numerical literature[16,17]. It includes a clock-ordered phase (see Fig. 1a) that breaks the C_6 symmetry of the triangular lattice for transverse field values below a critical threshold $\Delta < \Delta_c$ and below a Berezinskii–Kosterlitz–Thouless (BKT) transition temperature T_L. Above the clock-ordered phase, in the temperature range $T_L < T < T_U$, there exists a critical region characterized by power-law spin–spin correlations and an emergent XY symmetry.

To connect the generic physics of the model to the specific material TMGO, it is crucial to determine the corresponding TLI model

https://doi.org/10.1038/s41567-026-03304-5

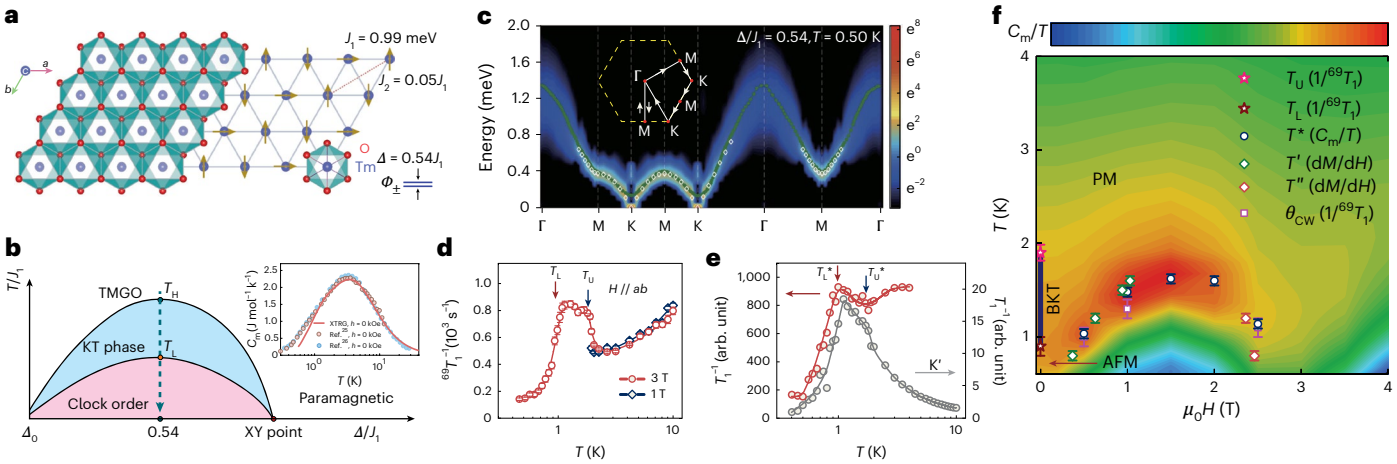

Fig. 1 | Triangular lattice Ising magnet TMGO. a, The Tm^{3+} ions have an energy splitting Δ between the two lowest non-Kramers electronic energy levels, labelled $\Phi_\pm$. These two levels constitute an effective spin-1/2 triangular-lattice Ising model on the triangular lattice, with nearest-neighbour and next-nearest-neighbour coupling parameters J_1 and J_2, respectively. An illustration of spin structure in the low-temperature clock phase of TMGO is provided, where the spin-up and spin-down arrows are along the out-of-plane magnetic easy c axis and the horizontal arrow illustrates spins in a superposition of spin-up and spin-down states. **b**, Schematic phase diagram of TLI model, as a function of temperature T and Δ normalized by J_1. The quantum critical point on the horizontal axis (red circle) has emergent spin XY symmetry, which extends into a BKT phase at finite T (blue region). The vertical arrowed line along $\Delta/J_1 = 0.54$ represents the relevant parameter range for TMGO, with two BKT transitions at T_L (orange circle) and T_U (blue circle). The inset shows specific-heat (C_m) measurements and their comparison with the exponential TRG (XTRG) computations for the triangular-lattice Ising model. This comparison was used to determine the optimal set of model parameters for QMC calculations[13]. **c**, QMC-calculated spin spectrum at $T = 0.5$ K (ref. 13). The computed spectrum agrees well with the experimental inelastic-neutron-scattering results taken from ref. 18, whose peak positions are shown as the green dotted line. **d**, NMR measurements of the ^{69}Ga spin relaxation rate $1/^{69}T_1$ versus T measured under in-plane magnetic fields H of 3 T and 1 T. A plateau feature, characterizing the anticipated BKT phase, is observed between $T_L \approx 0.9$ K and $T_U \approx 1.9$ K (ref. 19). **e**, QMC-computed $1/T_1$ data from the dynamical spin–spin correlation function with contributions from all momentum points in the Brillouin zone (left scale) and from momenta in the vicinity of the K′ Brillouin zone point (right scale)[19]. **f**, Experimental phase diagram of the material under an applied magnetic field. The solid vertical line illustrates the BKT phase between T_U and T_L, while the red arrow indicates the antiferromagnetic (AFM) clock order regime[17]. The temperatures corresponding to the maximum of the C_m/T (T^*) and the maximum of dM/dH (T''), where M is the material magnetization, and the Curie–Weiss temperature θ_{CW}, all collapse to the same phase boundary between the BKT-like regime and the AFM phase[19]. PM, paramagnetic. Panels reproduced from: **a**, ref. 13 under a Creative Commons license CC BY 4.0; **f**, ref. 19 under a Creative Commons license CC BY 4.0. Panels adapted from: **b**,**c**, ref. 13 under a Creative Commons license CC BY 4.0; **d**,**e**, ref. 19 under a Creative Commons license CC BY 4.0.

parameters—in particular, the ratio Δ/J_1. The availability of large-scale QMC and TRG calculations meant that numerical simulations of the specific heat and neutron-scattering spectrum could be quantitatively compared with experimental data (Fig. 1b inset and 1c). These comparisons were then used to precisely determine the model parameters of TMGO[13].

The extracted parameters placed TMGO in a region of the phase diagram with accessible clock and BKT phases, with $\Delta/J_1 = 0.54$. In contrast, simple mean-field calculations of the model estimated $\Delta/J_1 = 1.36$ (ref. 18) and would place the material in the disordered paramagnetic phase as $\Delta > \Delta_c \approx 0.8J_1$, the location of the quantum critical point. This suggests that the analytic mean-field treatment fails to capture quantum fluctuations intrinsic to the quantum TLI model and the material itself. The unbiased quantum many-body TRG+QMC scheme is necessary to explain the observed inelastic-neutron-scattering spectrum.

Furthermore, the QMC simulations of the TLI model in equation (1), for Hamiltonian parameters determined in ref. 13, quantitatively predicted the existence of a BKT phase between the high-temperature disordered phase and a low-temperature antiferromagnetic phase. This predicted phase was later measured and confirmed using nuclear magnetic resonance (NMR)[19].

Comparisons between the observed NMR signal (Fig. 1d) and predictions using QMC (Fig. 1e) demonstrate that the numerical data match NMR experiments.

This TLI case study underscores the power of combining experimental input with controlled many-body methods to refine and validate microscopic models. Theoretical insights into the BKT phase, together with numerical methods for comparison with specific heat and inelastic neutron scattering, provide a coherent framework for interpreting the data. The experimentally guided numerical analysis then produced a prediction for the magnetic-field range of the finite-temperature BKT phase, leading to its observation using NMR. These elements converge to yield the complete phase diagram shown in Fig. 1f.

Triangular-lattice Heisenberg antiferromagnets

A longer-standing and more fundamental problem in quantum magnetism that highlights the need for a balanced and collaborative approach is the triangular-lattice Heisenberg antiferromagnet (TLHAF). The geometric frustration inherent to the lattice led to the proposal of the resonating valence bond spin-liquid state[20] over 50 years ago.

Although the nature of the TLHAF ground state remained a topic of debate for many years[21], a sequence of numerical works[22–24] has provided evidence in favour of 120° long-range magnetic order with a relatively small ordered moment (41% of the full moment)[24]. The reduction of the ordered moment indicates strong quantum fluctuations, which, in a semiclassical treatment, are reflected by large corrections to the magnetic excitation spectrum, including extensive decay of magnon excitations across much of the Brillouin zone[25,26].

In line with the proposal of a non-classical resonating valence bond state, early studies of the low-temperature properties of the TLHAF based on effective quantum field theories suggested the need for alternative descriptions beyond the semiclassical approach[27,28]. This was further supported by numerical work[29–34] on an extended model that includes J_1 and J_2 exchange interactions. These results indicate that a non-zero J_2 leads to a continuous quantum phase transition into a spin-liquid state at the quantum critical point $J_2/J_1 \approx 0.06$, as depicted in the phase diagram in Fig. 2a.

These studies prompted a series of inelastic-neutron-scattering experiments[35–38] on the quasi-two-dimensional nearest-neighbour

https://doi.org/10.1038/s41567-026-03304-5

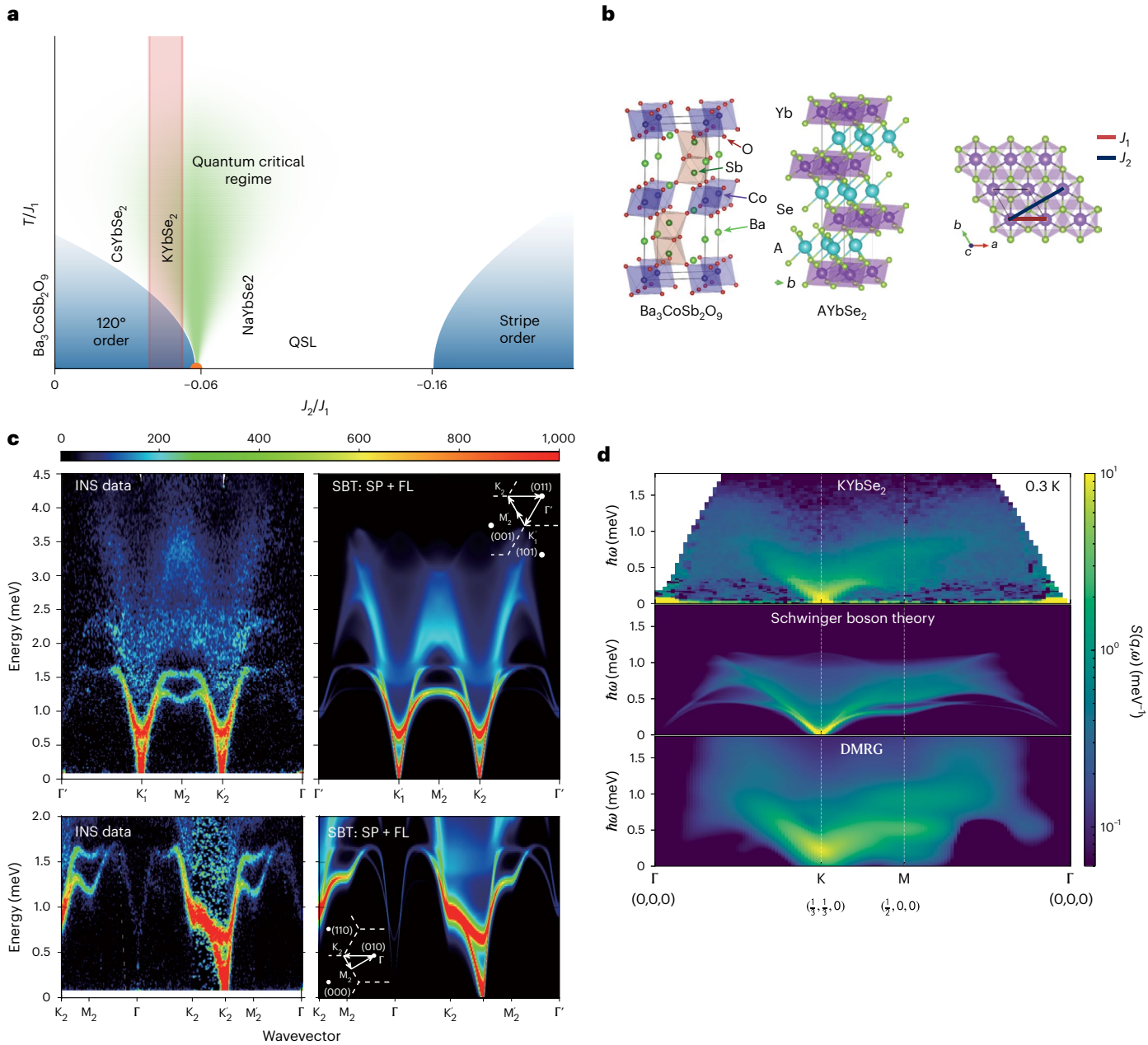

Fig. 2 | Triangular lattice Heisenberg antiferromagnets. a, Schematic phase diagram of the J_1–J_2 Heisenberg model based on numerical results[29–34] featuring a large quantum spin liquid (QSL) phase between two magnetically ordered phases (blue regions). The parameter regimes corresponding to several candidate materials are illustrated. **b**, Structure of the transition-metal oxide $Ba_3CoSb_2O_9$ and the Yb delafossite $AYbSe_2$, with A an alkali metal. **c**, Comparison between inelastic-neutron-scattering (INS) measurements of $Ba_3CoSb_2O_9$[38] (left) and the Schwinger boson theory (SBT) calculation, with saddle point (SP) plus fluctuations (FL), of the scattering cross-section[41] (right). The low-energy, sharply defined magnon modes are interpreted as two-spinon bound states, while the continuum scattering is dominated by the two-spinon continuum. The colour bar indicates intensity in arbitrary units. **d**, Comparison of inelastic-neutron-scattering data measured in $KYbSe_2$ with the dynamical spin structure factor obtained using Schwinger boson theory and DMRG calculations. Panels **a**, **b** and **d** reproduced with permission from ref. 43, Springer Nature. Panel **c** adapted with permission from: ref. 38, American Physical Society; ref. 41, American Physical Society.

TLHAF $Ba_3CoSb_2O_9$, shown in Fig. 2b, which revealed an anomalous scattering continuum and a strong renormalization of the single-magnon dispersion, confirming the expected breakdown of the semiclassical expansion due to proximity to the quantum critical point. In this regime, magnons should be described as bound states of two fractionalized spinons, which are the relevant quasiparticles in a spin-liquid state. At higher energies, the scattering continuum continuously evolves into the two-spinon continuum expected in a spin-liquid phase.

Large-N parton approaches for studying spin-liquid phases, where N denotes the number of parton flavours, are well suited to account for the continuum scattering in ordered phases close to a fractionalized phase, because their mean-field starting point corresponds to a free spinon gas. The Schwinger boson formalism[27,28,39] offers a natural framework where spinons, coupled through emergent gauge fields, are treated as bosons. This allows for a unified description of both ordered and spin-liquid phases. In this picture, long-range magnetic order arises from spontaneous condensation of the Schwinger bosons and magnon modes are obtained as two-spinon bound states induced by fluctuations of the gauge fields[40].

Because Schwinger boson theory is formulated on the lattice, it captures both short- and long-wavelength limits, enabling a comprehensive description of inelastic-neutron-scattering data. A comparison

https://doi.org/10.1038/s41567-026-03304-5

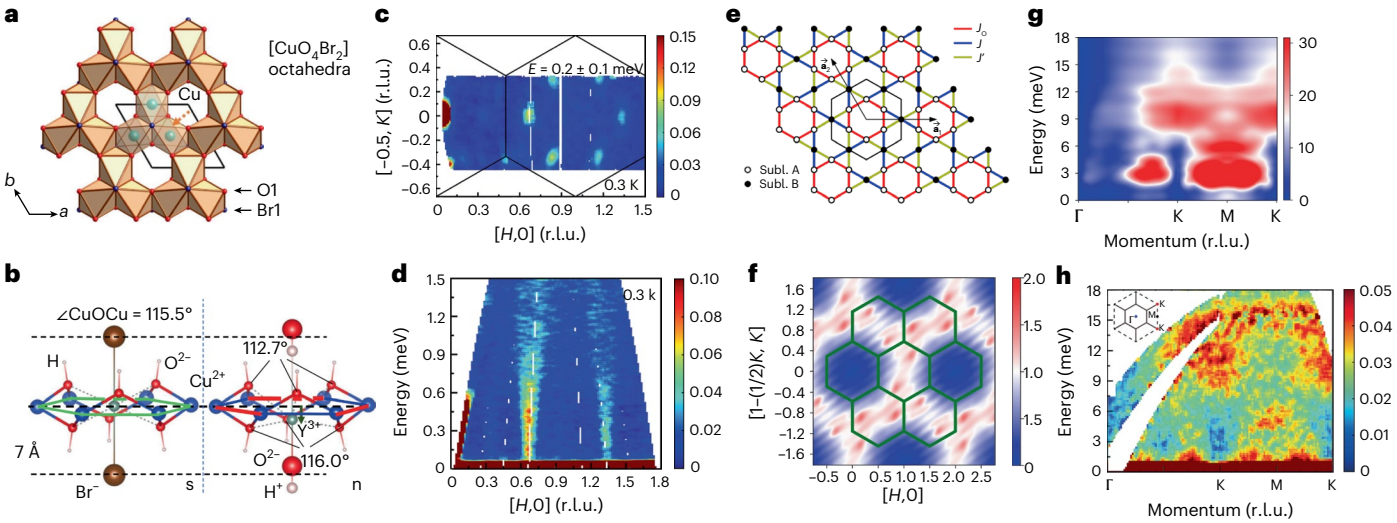

Fig. 3 | Kagome-lattice antiferromagnet YCu_3-Br. a, The structure of a kagome layer in YCu_3-Br, consisting of $[CuO_4Br_2]$ octahedra[62]. **b**, Optimized local structures for supercells containing symmetric (s) and non-symmetric (n) environments obtained from density functional theory calculations[11]. Y^{3+} ions reside at hexagonal centres but occupy two non-equivalent sites, one within and one displaced from the kagome planes. This positional distinction arises because some of the Br^- ions connecting Y^{3+} along the out-of-plane *c* axis are substituted by $(OH)^-$, which is polar and pulls the connected Y^{3+} ion out of the kagome plane. The different valences and ion sizes between Y^{3+} and Cu^{2+} help eliminate weakly correlated magnetic impurities often observed in herbertsmithite and related compounds due to partial substitution of Cu^{2+} ions on non-magnetic ions[53]. **c**,**d**, Intensity contour plots of the inelastic-neutron-scattering results in the [*H*, *K*] zone at 0.2 meV (**c**) and as a function of energy, *E*, and momentum, along the [*H*, 0] direction[60] (**d**). r.l.u., reciprocal lattice units. **e**, Schematic illustration of the 3*J* model used for classical spin-wave calculations[12], which introduces three different nearest-neighbour coupling constants between sites. Note that the unit cell of this model is three times larger than that of the kagome lattice, as represented by the black hexagon. **f**, The static spin structure factor *S*(*Q*) obtained from DMRG calculations as described in the text. The green hexagons depict the kagome Brillouin zone. **g**,**h**, Spin excitations from DMRG calculations (**g**) and inelastic-neutron-scattering measurements (**h**)[65]. The inset in **h** illustrates high-symmetry points in the kagome Brillouin zone. The colour bars in **c**, **d**, **g**, and **h** indicate intensity in arbitrary units. Panels reproduced with permission from: **a**, ref. 62, Elsevier; **c**,**d**, ref. 60, Springer Nature; **e**, ref. 12 under a Creative Commons license CC BY 4.0. Panels adapted with permission from: **b**, ref. 11, American Physical Society; **f**–**h**, ref. 65, American Physical Society.

with recent experiments[38,41] (which is reproduced in Fig. 2c) confirms that these calculations can accurately reproduce the magnon dispersion of $Ba_3CoSb_2O_9$, as well as the structure of the anomalous scattering continuum.

Following these findings, efforts to find TLHAF quantum spin liquids[42–44] have compared inelastic-neutron-scattering data from a series of Yb delafossites, $AYbSe_2$ (A being an alkali metal), with tunable J_2/J_1 ratios, with state-of-the-art calculations of the dynamical spin structure factor using both DMRG and Schwinger boson calculations (see Fig. 2d). Access to these state-of-the-art computational methods—and their agreement with observations—plays a crucial role in interpreting complicated neutron-scattering spectra. Here again, advanced analytic theory and the large-scale quantum many-body simulation work with experiments in an integrated manner.

One such study[44] recently reported that $NaYbSe_2$ exhibits no detectable phase transition down to the base temperature of the experiment. Unfortunately, it would be premature to draw definitive conclusions about the ground state, as the mobility of Na ions can introduce structural and magnetic disorder[45], potentially obscuring intrinsic quantum behaviour.

However, if a robust realization of a spin liquid is confirmed, there remains the challenge of identifying its character among many competing theoretical scenarios. The observation of a low-energy spin gap in the inelastic-neutron-scattering spectrum would rule out a gapless $\mathbb{U}(1)$ Dirac quantum spin liquid[29,32]. Nonetheless, several distinct gapped phases have been proposed for the triangular lattice: a resonating valence bond (gapped $\mathbb{Z}_2$) spin liquid[46–48], a valence bond crystal[49,50] and a chiral quantum spin liquid[51].

Both the chiral quantum spin liquid and the valence bond crystal break discrete symmetries—time-reversal and lattice symmetries, respectively—and therefore must exhibit finite-temperature phase transitions to restore these symmetries at higher temperature. In contrast, the $\mathbb{Z}_2$ spin liquid preserves all symmetries and does not undergo such a transition. The characteristic of the $\mathbb{U}(1)$ Dirac quantum spin liquid, on the other hand, is a gapless continuum at the K and M points of the Brillouin zone.

This rational approach—combining high-resolution inelastic-neutron-scattering measurements with advanced numerical and analytical techniques—is proving highly effective in guiding the search for extreme quantum states of matter, such as spin liquids. In particular, it provides direct evidence for the proximity to, or presence of, fractionalization, which is essential for identifying and characterizing these phases.

As well as providing support for experimental claims of spin-liquid behaviour, numerical calculations are also increasingly playing a role in ruling out spin-liquid candidates. For example, the combination of ground-state phase diagram calculations using DMRG[34] and ultralow-temperature alternating-current susceptibility measurements[52] revealed that $YbZnGaO_4$, previously proposed as a triangular-lattice spin-liquid candidate, is in fact in a spin-glass state.

Kagome-lattice Heisenberg antiferromagnets

One of the most challenging issues in frustrated quantum magnetism is understanding the kagome-lattice Heisenberg antiferromagnet. This model has been a long-term candidate quantum spin liquid[53]. Despite extensive theoretical modelling, large-scale simulations, and experimental investigations, however, no consensus has emerged on whether any specific material definitively realizes a quantum spin-liquid state, and if so which kind, even for the simplest model with only nearest-neighbour exchange interactions.

This debate extends to key kagome quantum spin-liquid candidates, such as herbertsmithite and $Cu_3Zn(OH)_6FBr$[54–56]. However, progress is hindered by intrinsic magnetic impurities from a small percentage of Cu^{2+} ions on non-magnetic sites. It is complicated to

disentangle impurity effects from the intrinsic low-energy excitations that would reflect spin-liquid behaviour[57,58].

Beyond impurity effects, direct comparisons between theory and experiment remain difficult, as real materials typically include additional, non-Heisenberg interactions beyond the theoretical ideal modes, and their high-energy spin excitations are rarely observed due to the weak signal of the broad excitations, adding complexity to theoretical calculations.

Following advances in material synthesis and experimental methods, possible evidence for gapless, linearly dispersing Dirac spinons has been identified in $YCu_3(OH)_6Br_2[Br_{1-x}(OH)_x]$ (YCu_3-Br)[59–61]. The YCu_3-Br structure consists of ideal kagome planes formed by Cu^{2+} ions, each of which is surrounded by four equatorial O^- and two apical Br^- (B1) anions, forming a $[CuO_4Br_2]$ octahedron, shown in Fig. 3a ref. 62.

These developments offer a fresh direction to address long-standing questions in the study of kagome Heisenberg antiferromagnets.

Many studies of YCu_3-Br have demonstrated the absence of magnetic ordering down to 50 mK (refs. 59,62). Evidence for Dirac spinons emerged in specific-heat results, which display a T^2 dependence at zero field and an additional linear term at high magnetic fields[59]. These behaviours align with mean-field predictions for a $\mathbb{U}(1)$ Dirac quantum spin liquid[63]. Raman spectra further reveal broad magnetic excitations at high energies, attributed to one pair and two pairs of spinon–antispinon excitations[61]. The sublinear power-law dependence of the Raman susceptibility on energy also suggests Dirac spinons at high energies.

More compelling evidence arises from inelastic neutron scattering[60], which shows a conical spin continuum at low energies (Fig. 3c,d). The width of these spin excitations demonstrates a precise linear dependence on energy, consistent with a Dirac spinon cone centred at or near zero energy. Notably, the estimated spinon velocity accurately reproduces the low-temperature specific heat without further parameter adjustments.

These features differ markedly from semiclassical spin-wave calculations, where introducing strong randomness to generate a continuum-like spectra broadens low-energy spin excitations and reduces their central intensity[64]. Crucially, a damped spin-wave model cannot account for the substantial intensity observed in neutron-scattering spectra at the two-dimensional kagome Brillouin zone point (1/3, 0) due to the structure-factor constraints[65].

Although YCu_3-Br possesses an ideal Cu^{2+} kagome lattice, the location of its spin excitations in momentum space, as measured by neutron scattering, cannot be reproduced by conventional Heisenberg models. This discrepancy arises from the distorted local structure (Fig. 3b), which generates two distinct hexagonal structures. Consequently, three different nearest exchange interactions emerge.

The observed quantum-spin-liquid-like behaviour emerges when the proportion of one of these structures reaches around two-thirds (ref. 66). Furthermore, the sharp low-energy spin excitations of YCu_3-Br demonstrate that the two local structures are not randomly distributed.

In a similar material, $Y_3Cu_9(OH)_{19}Cl_8$ (Y_3Cu_9-Cl), the two hexagonal structures arrange in an ordered pattern, forming a kagome superlattice with threefold enlarged unit-cell area[64]. YCu_3-Br and Y_3Cu_9-Cl exhibit identical low-energy magnetic excitation wavevectors despite the latter forming an antiferromagnetically ordered phase[64], indicating that they necessitate comparable theoretical descriptions.

Ab initio density-functional-theory calculations have identified three distinct nearest-neighbour superexchange interactions in Y_3Cu_9-Cl[12]. A classical spin-wave analysis of the kagome Heisenberg model incorporating these couplings (Fig. 3e), known as the 3J model, captures the antiferromagnetic order observed in Y_3Cu_9-Cl[12,64]. Yet this description departs from the ideal kagome Heisenberg limit, as the arrangement of the distortions breaks translational symmetry.

This raises several theoretical and computational challenges. Given the similarities between YCu_3-Br and Y_3Cu_9-Cl, there is hope that, starting from a common theoretical model of the two compounds, ab initio methods, DMRG, QMC and field-theoretical approaches, such as Schwinger boson techniques, that account for strong quantum fluctuations may be able to identify a possible transition from antiferromagnetic order to a quantum spin liquid. This should make it possible to track the evolution of fractionalized excitations even when the ground state is not a spin liquid, providing essential guidance for experiments.

The freedom to explore theoretical parameter space might also make it possible to search for a quantum spin liquid as a stable intermediate phase on the path from the Y_3Cu_9-Cl structure with hexagonal distortions towards the theoretical ideal homogeneous kagome Heisenberg antiferromagnet[63,67–69]. At present, fundamental questions remain open and call for systematic exploration.

An initial integrated numerical study of the 3J model—combining classical Landau–Lifshitz dynamics with DMRG time evolution—has already succeeded in reproducing the static structure factor (Fig. 3f) and the high-energy spectral features (Fig. 3g,h) observed experimentally[65]. The influence of the Dzyaloshinskii–Moriya interaction on the low-energy spin excitations has likewise been examined using DMRG, and the results capture the enhanced in-plane magnetic fluctuations revealed by recent polarized neutron-scattering measurements[65].

This agreement reinforces the validity of the 3J model and highlights the need for more advanced computational approaches to resolve the remaining low-energy excitation spectrum. Intriguingly, similar spin-liquid behaviour in specific-heat measurements at zero and finite magnetic field has also been reported in $LuCu_3(OH)_6Br_2[Br_{0.33}(OH)_{0.67}]$ ($LuCu_3$-Br)[70], which shares the same nuclear structure as Y_3Cu_9-Cl. On the other hand, $LuCu_3$-Br does not have the randomness of the two local hexagonal structures present in YCu_3-Br. This demonstrates that randomness or disorder is not a necessary ingredient for realizing quantum spin-liquid physics within this family of models.

Discussion

The three examples highlighted here mark recent milestones in quantum magnetism and underscore a common theme: progress emerges from a balanced integration of advanced numerical simulations, field-theoretical analysis and materials synthesis and characterization. This collaborative framework moves beyond the outdated view that one pillar—such as predictions from a toy model—drives discovery whereas the others merely validate it. Instead, it affirms their equal importance in advancing our understanding of quantum materials.

TRG techniques, augmented with state-of-the-art ab initio methods, now allow simulations of realistic spin model Hamiltonians on cylindrical geometries. This capability enables access to thermodynamic properties, such as magnetic susceptibility and specific heat, for quantitative comparisons with experimental data. Furthermore, these comparisons with experimental data can be refined into an iterative scheme, where optimized model parameters are determined through automated, machine-learning-based software, paving the way for more precise and efficient model fitting.

Most tensor-network calculations of spectra and thermodynamic properties are still performed using a quasi-one-dimensional cylindrical geometry in DMRG, as this is the only setting in which the scaling of the needed computational resources with system size can still be controlled. However, the limitations of this approach, and the need to perform true two-dimensional tensor-network renormalization group calculations, have become more and more obvious, if we want to have good momentum resolution in the two-dimensional Brillouin zone. Achieving this with acceptable accuracy and an affordable computation burden would enable a much more detailed comparison between experiment and model calculations, substantially strengthening the integrated approach.

With access to optimized model parameters, QMC simulations can then compute the partition function of fully optimized two-dimensional lattice model Hamiltonians and access all dynamical and thermodynamic correlation functions with lower computational

complexity, and access to both ground-state and finite temperatures that is difficult to achieve using tensor-network methods. Until recently, QMC methods were limited by their reliance on imaginary-time data in the path-integral framework, which cannot be directly compared with real-time or frequency-dependent experimental data. However, this limitation has been effectively addressed by the stochastic analytic continuation technique[6], which transforms a laborious search for the optimized spectrum in an exponentially large space into a structured, importance-sampling Monte Carlo process. This procedure allows QMC to yield real-frequency dynamic spectra that can be directly compared with inelastic neutron scattering and NMR experimental results[13,17,19].

In the future, better lattice models are needed so that QMC simulations can capture the complex physics of real materials, including multiple interactions and geometric frustration. Most direct implementations of these properties with QMC will encounter the minus-sign problem, or very long autocorrelation times in the update scheme, making calculations intractable. We need to find effective models that capture the essential physics of the material and yet remain numerically manageable using QMC.

One recent advance in this direction is the ability to directly simulate emergent gauge fields coupled to fractionalized excitations on the lattice[71]. Such simulations can provide valuable insight into quantum spin-liquid physics across a range of temperatures and magnetic fields, offering a powerful framework for guiding and interpreting experiments.

The success of the Schwinger boson formalism in interpreting the inelastic-neutron-scattering spectra of $Ba_3CoSb_2O_9$[38,41] demonstrates the continued power of analytical methods. Although parton theories can capture key features of spectroscopic measurements, going beyond mean-field theory is crucial to accurately describe both the collective modes and the broad scattering continuum on the magnetically ordered side.

More advanced Schwinger boson calculations already incorporate low-order contributions from gauge-field fluctuations[40,41]. This extension has led to improved agreement with experimental data, indicating that the systematic inclusion of higher-order fluctuation contributions is a promising direction for further development. More generally, within large-N parton frameworks, incorporating fluctuations beyond the mean-field approximation is essential for describing collective modes with integer spin and, more broadly, for achieving an accurate characterization of dynamical correlations[72].

One of the biggest challenges facing the field of quantum magnetism, which we have not yet discussed, is the ongoing search for Kitaev quantum spin liquids. Following Alexei Kitaev's exact solution of the honeycomb model[73], substantial effort has gone into identifying materials that might realize this physics[74], with candidates including various iridates and ruthenates[75].

Despite extensive research into these candidate materials, the details of the appropriate spin Hamiltonians to capture their behaviour remain elusive[76,77]. This uncertainty stems from multiple factors. For example, the theoretically ideal Kitaev interaction is often accompanied by additional anisotropic exchange terms. The magnetism in the candidate materials arises from 4*d* and 5*d* orbital electrons, whose spatial extent introduces further-neighbour couplings. Furthermore, there is evidence that accurate modelling of the electronic structure may require more careful treatment of the hybridization between ligand and metal orbitals than has been performed so far.

Given the large number of symmetry-allowed interaction terms, a reliable extraction of the effective spin model requires a multitarget approach that synthesizes different experimental observables with predictive many-body simulations[76,77]. As it stands, the Kitaev model is a beautiful but abstract example of emergent gauge theories in spin systems. Absent a comprehensive strategy anchored in both experiment and computation, it may remain as speculative as the original lattice gauge theories of high-energy physics[78].

This is where the more integrated approach we advocate in this Perspective could improve the situation. Ab initio methods and TRG can be iteratively compared with thermodynamic measurements to determine the precise model parameters. With access to an effective model, more accurate techniques such as QMC can be used to make quantitative comparisons with inelastic-neutron-scattering results. In this way, the successes achieved in the three examples could be replicated to advance the study of Kitaev physics.

We encourage the community to adopt a balanced perspective in which advanced numerical simulations, cutting-edge field theory and innovative materials synthesis and characterization operate in concert rather than in hierarchy. Such integration is essential for uncovering deeper insights into quantum systems and, ultimately, for achieving the long-sought experimental breakthroughs needed to establish quantum spin liquids conclusively.

References

1. Haldane, F. D. M. 'Luttinger liquid theory' of one-dimensional quantum fluids. I. Properties of the Luttinger model and their extension to the general 1D interacting spinless Fermi gas. *J. Phys. C* **14**, 2585–2610 (1981).
2. Lake, B., Tennant, D. A., Frost, C. D. & Nagler, S. E. Quantum criticality and universal scaling of a quantum antiferromagnet. *Nat. Mater.* **4**, 329–334 (2005).
3. Coldea, R. et al. Quantum criticality in an Ising chain: experimental evidence for emergent E_8 symmetry. *Science* **327**, 177–180 (2010).
4. Lake, B., Tennant, D. A., Frost, C. D. & Nagler, S. E. Quantum criticality and universal scaling of a quantum antiferromagnet. *Phys. Rev. Lett.* **111**, 137205 (2013).
5. Mourigal, M. et al. Fractional spinon excitations in the quantum Heisenberg antiferromagnetic chain. *Nat. Phys.* **9**, 435–441 (2013).
6. Shao, H. et al. Nearly deconfined spinon excitations in the square-lattice spin-1/2 Heisenberg antiferromagnet. *Phys. Rev. X* **7**, 041072 (2017).
7. Haegeman, J., Lubich, C., Oseledets, I., Vandereycken, B. & Verstraete, F. Unifying time evolution and optimization with matrix product states. *Phys. Rev. B* **94**, 165116 (2016).
8. Savary, L. & Balents, L. Quantum spin liquids: a review. *Rep. Prog. Phys.* **80**, 016502 (2017).
9. Knolle, J. & Moessner, R. A field guide to spin liquids. *Annu. Rev. Condens. Matter Phys.* **10**, 451–472 (2019).
10. Villanova, J. W., Scheie, A. O., Tennant, D. A., Okamoto, S. & Berlijn, T. First-principles derivation of magnetic interactions in the triangular quantum spin liquid candidates $KYbCh_2$ (Ch = S, Se, Te) and $AYbSe_2$ (A = Na, Rb). *Phys. Rev. Res.* **5**, 033050 (2023).
11. Liu, J. et al. Gapless spin liquid behavior in a kagome Heisenberg antiferromagnet with randomly distributed hexagons of alternate bonds. *Phys. Rev. B* **105**, 024418 (2022).
12. Hering, M. et al. Phase diagram of a distorted kagome antiferromagnet and application to Y-kapellasite. *npj Comput. Mater.* **8**, 10 (2022).
13. Li, H. et al. Kosterlitz–Thouless melting of magnetic order in the triangular quantum Ising material $TmMgGaO_4$. *Nat. Commun.* **11**, 1111 (2020).
14. Cevallos, F. A., Stolze, K., Kong, T. & Cava, R. Anisotropic magnetic properties of the triangular plane lattice material $TmMgGaO_4$. *Mater. Res. Bull.* **105**, 154–158 (2018).
15. Li, Y. et al. Partial up–up–down order with the continuously distributed order parameter in the triangular antiferromagnet $TmMgGaO_4$. *Phys. Rev. X* **10**, 011007 (2020).
16. Isakov, S. V. & Moessner, R. Interplay of quantum and thermal fluctuations in a frustrated magnet. *Phys. Rev. B* **68**, 104409 (2003).

17. Da Liao, Y. et al. Phase diagram of the quantum Ising model on a triangular lattice under external field. *Phys. Rev. B* **103**, 104416 (2021).
18. Shen, Y. et al. Intertwined dipolar and multipolar order in the triangular-lattice magnet $TmMgGaO_4$. *Nat. Commun.* **10**, 4530 (2019).
19. Hu, Z. et al. Evidence of the Berezinskii–Kosterlitz–Thouless phase in a frustrated magnet. *Nat. Commun.* **11**, 5631 (2020).
20. Anderson, P. Resonating valence bonds: a new kind of insulator?. *Mater. Res. Bull.* **8**, 153–160 (1973).
21. Zheng, W., Fjærestad, J. O., Singh, R. R. P., McKenzie, R. H. & Coldea, R. Excitation spectra of the spin-½ triangular-lattice Heisenberg antiferromagnet. *Phys. Rev. B* **74**, 224420 (2006).
22. Huse, D. A. & Elser, V. Simple variational wave functions for two-dimensional Heisenberg spin-s=½ J_1–J_2 antiferromagnets. *Phys. Rev. Lett.* **60**, 2531–2534 (1988).
23. Bernu, B., Lhuillier, C. & Pierre, L. Signature of Néel order in exact spectra of quantum antiferromagnets on finite lattices. *Phys. Rev. Lett.* **69**, 2590–2593 (1992).
24. Capriotti, L., Trumper, A. E. & Sorella, S. Long-range Néel order in the triangular Heisenberg model. *Phys. Rev. Lett.* **82**, 3899–3902 (1999).
25. Starykh, O. A., Chubukov, A. V. & Abanov, A. G. Flat spin-wave dispersion in a triangular antiferromagnet. *Phys. Rev. B* **74**, 180403 (2006).
26. Zhitomirsky, M. E. & Chernyshev, A. L. Colloquium: Spontaneous magnon decays. *Rev. Mod. Phys.* **85**, 219–242 (2013).
27. Read, N. & Sachdev, S. Large-n expansion for frustrated quantum antiferromagnets. *Phys. Rev. Lett.* **66**, 1773–1776 (1991).
28. Chubukov, A. V., Sachdev, S. & Senthil, T. Quantum phase transitions in frustrated quantum antiferromagnets. *Nucl. Phys. B* **426**, 601–643 (1994).
29. Kaneko, R., Morita, S. & Imada, M. Gapless spin-liquid phase in an extended spin 1/2 triangular Heisenberg model. *J. Phys. Soc. Jpn.* **83**, 093707 (2014).
30. Zhu, Z. & White, S. R. Spin liquid phase of the S=½ J_1–J_2 Heisenberg model on the triangular lattice. *Phys. Rev. B* **92**, 041105 (2015).
31. Hu, W.-J., Gong, S.-S., Zhu, W. & Sheng, D. N. Competing spin-liquid states in the spin-½ Heisenberg model on the triangular lattice. *Phys. Rev. B* **92**, 140403 (2015).
32. Iqbal, Y., Hu, W.-J., Thomale, R., Poilblanc, D. & Becca, F. Spin liquid nature in the Heisenberg J_1–J_2 triangular antiferromagnet. *Phys. Rev. B* **93**, 144411 (2016).
33. Saadatmand, S. N. & McCulloch, I. P. Symmetry fractionalization in the topological phase of the spin-½ J_1–J_2 triangular Heisenberg model. *Phys. Rev. B* **94**, 121111 (2016).
34. Zhu, Z., Maksimov, P. A., White, S. R. & Chernyshev, A. L. Topography of spin liquids on a triangular lattice. *Phys. Rev. Lett.* **120**, 207203 (2018).
35. Ma, J. et al. Static and dynamical properties of the spin-1/2 equilateral triangular-lattice antiferromagnet $Ba_3CoSb_2O_9$. *Phys. Rev. Lett.* **116**, 087201 (2016).
36. Ito, S. et al. Structure of the magnetic excitations in the spin-1/2 triangular-lattice Heisenberg antiferromagnet $Ba_3CoSb_2O_9$. *Nat. Commun.* **8**, 235 (2017).
37. Kamiya, Y. et al. The nature of spin excitations in the one-third magnetization plateau phase of $Ba_3CoSb_2O_9$. *Nat. Commun.* **9**, 2666 (2018).
38. Macdougal, D. et al. Avoided quasiparticle decay and enhanced excitation continuum in the spin-½ near-Heisenberg triangular antiferromagnet $Ba_3CoSb_2O_9$. *Phys. Rev. B* **102**, 064421 (2020).
39. Arovas, D. P. & Auerbach, A. Functional integral theories of low-dimensional quantum Heisenberg models. *Phys. Rev. B* **38**, 316–332 (1988).
40. Ghioldi, E. A. et al. Dynamical structure factor of the triangular antiferromagnet: Schwinger boson theory beyond mean field. *Phys. Rev. B* **98**, 184403 (2018).
41. Ghioldi, E. A. et al. Evidence of two-spinon bound states in the magnetic spectrum of $Ba_3CoSb_2O_9$. *Phys. Rev. B* **106**, 064418 (2022).
42. Xie, T. et al. Complete field-induced spectral response of the spin-1/2 triangular-lattice antiferromagnet $CsYbSe_2$. *npj Quantum Mater.* **8**, 48 (2023).
43. Scheie, A. O. et al. Proximate spin liquid and fractionalization in the triangular antiferromagnet $KYbSe_2$. *Nat. Phys.* **20**, 74–81 (2024).
44. Scheie, A. O. et al. Spectrum and low-energy gap in triangular quantum spin liquid $NaYbSe_2$. Preprint at https://arxiv.org/html/2406.17773 (2024).
45. Lyu, Y. et al. Entanglement randomness and gapped itinerant carriers in a frustrated quantum magnet. *Phys. Rev. X* **15**, 041035 (2025).
46. Sachdev, S. Kagomé- and triangular-lattice Heisenberg antiferromagnets: ordering from quantum fluctuations and quantum-disordered ground states with unconfined bosonic spinons. *Phys. Rev. B* **45**, 12377–12396 (1992).
47. Wang, F. & Vishwanath, A. Spin-liquid states on the triangular and kagomé lattices: a projective-symmetry-group analysis of Schwinger boson states. *Phys. Rev. B* **74**, 174423 (2006).
48. Shackleton, H. & Sachdev, S. Sign-problem-free effective models of triangular lattice quantum antiferromagnets. *Phys. Rev. B* **111**, 075101 (2025).
49. Miksch, B. et al. Gapped magnetic ground state in quantum spin liquid candidate κ-$(BEDT\text{-}TTF)_2Cu_2(CN)_3$. *Science* **372**, 276–279 (2021).
50. Seifert, U. F. P., Willsher, J., Drescher, M., Pollmann, F. & Knolle, J. Spin-Peierls instability of the U(1) Dirac spin liquid. *Nat. Commun.* **15**, 7110 (2024).
51. Szasz, A., Motruk, J., Zaletel, M. P. & Moore, J. E. Chiral spin liquid phase of the triangular lattice Hubbard model: a density matrix renormalization group study. *Phys. Rev. X* **10**, 021042 (2020).
52. Ma, Z. et al. Spin-glass ground state in a triangular-lattice compound $YbZnGaO_4$. *Phys. Rev. Lett.* **120**, 087201 (2018).
53. Norman, M. R. Colloquium: Herbertsmithite and the search for the quantum spin liquid. *Rev. Mod. Phys.* **88**, 041002 (2016).
54. Han, T.-H. et al. Fractionalized excitations in the spin-liquid state of a kagome-lattice antiferromagnet. *Nature* **492**, 406–410 (2012).
55. Feng, Z. et al. Gapped spin-1/2 spinon excitations in a new kagome quantum spin liquid compound $Cu_3Zn(OH)_6FBr$. *Chin. Phys. Lett.* **34**, 077502 (2017).
56. Khuntia, P. et al. Gapless ground state in the archetypal quantum kagome antiferromagnet $ZnCu_3(OH)_6Cl_2$. *Nat. Phys.* **16**, 469–474 (2020).
57. Nilsen, G. J., de Vries, M. A., Stewart, J. R., Harrison, A. & Rønnow, H. M. Low-energy spin dynamics of the s=1/2 kagome system herbertsmithite. *J. Phys.: Condens. Matter* **25**, 106001 (2013).
58. Wei, Y. et al. Nonlocal effects of low-energy excitations in quantum-spin-liquid candidate $Cu_3Zn(OH)_6FBr$. *Chin. Phys. Lett.* **38**, 097501 (2021).
59. Zeng, Z. et al. Possible Dirac quantum spin liquid in the kagome quantum antiferromagnet $YCu_3(OH)_6Br_2[Br_x(OH)_{1-x}]$. *Phys. Rev. B* **105**, L121109 (2022).
60. Zeng, Z. et al. Spectral evidence for Dirac spinons in a kagome lattice antiferromagnet. *Nat. Phys.* **20**, 1097–1102 (2024).
61. Jeon, S. et al. One-ninth magnetization plateau stabilized by spin entanglement in a kagome antiferromagnet. *Nat. Phys.* **20**, 435–441 (2024).

62. Chen, X.-H., Huang, Y.-X., Pan, Y. & Mi, J.-X. Quantum spin liquid candidate $YCu_3(OH)_6Br_2[Br_x(OH)_{1-x}]$ ($x \approx 0.51$): with an almost perfect kagomé layer. *J. Magn. Magn. Mater.* **512**, 167066 (2020).
63. Ran, Y., Hermele, M., Lee, P. A. & Wen, X.-G. Projected-wave-function study of the spin-1/2 Heisenberg model on the kagomé lattice. *Phys. Rev. Lett.* **98**, 117205 (2007).
64. Chatterjee, D. et al. From spin liquid to magnetic ordering in the anisotropic kagome Y-kapellasite $Y_3Cu_9(OH)_{19}Cl_8$: a single-crystal study. *Phys. Rev. B* **107**, 125156 (2023).
65. Han, L. et al. Spin excitations arising from anisotropic Dirac spinons in $YCu_3(OD)_6Br_2[Br_{0.33}(OD)_{0.67}]$. *Phys. Rev. B* **112**, 045114 (2025).
66. Xu, A. et al. Magnetic ground states in the kagome system $YCu_3(OH)_6[(Cl_xBr_{1-x})_{3-y}(OH)_y]$. *Phys. Rev. B* **110**, 085146 (2024).
67. Yan, S., Huse, D. A. & White, S. R. Spin-liquid ground state of the s=1/2 kagome Heisenberg antiferromagnet. *Science* **332**, 1173–1176 (2011).
68. Depenbrock, S., McCulloch, I. P. & Schollwöck, U. Nature of the spin-liquid ground state of the *s* = 1/2 Heisenberg model on the kagome lattice. *Phys. Rev. Lett.* **109**, 067201 (2012).
69. Liao, H. J. et al. Gapless spin-liquid ground state in the *s* = 1/2 kagome antiferromagnet. *Phys. Rev. Lett.* **118**, 137202 (2017).
70. Li, Z. et al. Antiferromagnetic order and possible quantum spin liquid in kagome antiferromagnet $LuCu_3(OH)_6Br_2[Br_x(OH)_{1-x}]$. *Chin. Phys. Lett.* **42**, 027504 (2025).
71. Xu, X. Y. et al. Monte Carlo study of lattice compact quantum electrodynamics with fermionic matter: the parent state of quantum phases. *Phys. Rev. X* **9**, 021022 (2019).
72. Willsher, J. & Knolle, J. Dynamics and stability of U(1) spin liquids beyond mean-field theory: triangular-lattice J_1–J_2 Heisenberg model. Preprint at https://arxiv.org/abs/2503.13831 (2025).
73. Kitaev, A. Anyons in an exactly solved model and beyond. *Ann. Phys. (N. Y.)* **321**, 2–111 (2006).
74. Jackeli, G. & Khaliullin, G. Mott insulators in the strong spin–orbit coupling limit: from Heisenberg to a quantum compass and Kitaev models. *Phys. Rev. Lett.* **102**, 017205 (2009).
75. Trebst, S. & Hickey, C. Kitaev materials. *Phys. Rep.* **950**, 1–37 (2022).
Comprehensive theoretical and experimental review of Kitaev materials.
76. Möller, M. et al. Rethinking α-$RuCl_3$: parameters, models, and phase diagram. *Phys. Rev. B* **112**, 104403 (2025).
77. Matsuda, Y., Shibauchi, T. & Kee, H.-Y. Kitaev quantum spin liquids. *Rev. Mod. Phys.* **97**, 045003 (2025).
78. Kogut, J. B. An introduction to lattice gauge theory and spin systems. *Rev. Mod. Phys.* **51**, 659–713 (1979).

Acknowledgements

Z.Y.M. thanks C. Zhou for help with creating the figures and acknowledges support from the Research Grants Council (RGC) of Hong Kong (projects AoE/P701/20, C7037-22GF, 17302223, 17301924, 17301725), the ANR/RGC Joint Research Scheme sponsored by the RGC of Hong Kong and French National Research Agency (project A_HKU703/22) and the State Key Laboratory of Optical Quantum Materials at HKU. We thank the HPC2021 system under Information Technology Services and the Blackbody high-performance computing system at the Department of Physics, University of Hong Kong, as well as the Beijing PARATERA Tech Co., Ltd. (https://cloud.paratera.com), for providing high-performance computing resources that have contributed to the research results reported within this paper. C.D.B. acknowledges support by the US Department of Energy, Office of Science, National Quantum Information Science Research Centers, Quantum Science Center. S.L. acknowledges support from the National Key Research and Development Program of China (grants 2022YFA1403400, 2021YFA1400400) and the Chinese Academy of Sciences (grants XDB33000000, GJTD-2020-01). Z.Y.M. and C.D.B. are grateful to the Pollica Physics Centre for hospitality during the stimulating workshop 'Exotic quantum matter: from quantum spin liquids to novel field theories' (2024).

Author contributions

Z.Y.M. and C.D.B. conceived the content and structure of the paper and all three authors contributed to the writing and discussion of the paper.

Competing interests

The authors declare no competing interests.

Additional information

Correspondence should be addressed to Zi Yang Meng, Cristian D. Batista or Shiliang Li.

Peer review information *Nature Physics* thanks the anonymous reviewers for their contribution to the peer review of this work.